Assessing Structural Integrity of Titanium-Based Alloy Brackets with Flaws Using Franc3D

by

Priscilla L. Chin

A Engineering Project Submitted to the Graduate

Faculty of Rensselaer Polytechnic Institute

in Partial Fulfillment of the

Requirements for the degree of

MASTER OF MECHANICAL ENGINEERING

Approved:

____

Ernesto Gutierrez-Miravete, Project Adviser

Rensselaer Polytechnic Institute
Hartford, Connecticut

April 2011
(For Graduation May 2011)

CONTENTS

LIST OF TABLES

LIST OF FIGURES

ACKNOWLEDGMENT

Many thanks to Professor Ernesto Gutierrez-Miravete for his guidance and advice; Valeriy Krutiy for information on resources; Michael R. Thomas for contributing his bracket geometry for this paper.

ABSTRACT

Given limited engine design space, engineers strive to optimize bracket geometry to produce high efficient and high performance engines that will operate at minimum weight and cost. Engineers often look to shave materials from bracket and design the thinnest possible brackets. Although this method could reduce weight, but brittle issues often found in bulk materials that could cause early failures in the structure. The focus of this paper is on assessing the structural integrity of Ti-6Al-4V bracket, which contains physical flaws or material imperfections. The structural flaws or material imperfections often observed in the corner and at the material surface, thus a circular crack was placed at the corner and on the surface of the material. Stresses in the vicinity of the crack tip were analyzed by ANSYS and the stress-intensity factors, computed by FRANC3D, were compared against material toughness to determine the structural integrity of the bracket.

1. Introduction/Literature Review

Airliners progressively more demand for high performance and fuel-efficient aircrafts due to the increasing gasoline price. In order to meet the market needs, original equipment manufacturers are developing smaller and lighter aircraft engines. Industry analysts are expecting the engine components in the next decades to be very space efficient. As a result, light but high strength materials are very valuable and competitively sourced to reduce weight and cost in manufacturing aircraft engine.

Aero engine designers design brackets in various shapes and sizes for mounting bleed air ducting, starter air duct, fuel lines and hydraulic lines to the engine core. One can find more than one hundred mounting points in an engine. Many of the ducting supports have the shapes of L, T and Z (multiple bends) to accommodate multiple tubes in the tight space found in an aircraft engine. In general, the bracket thickness ranges from .125 to .500 inch because the brackets not only must be thin to reduce weight and cost, but also must be functional and serve its purposes in the extreme environment, e.g. extremely high temperature, combination of vibration load, bending moment and maneuver load. Any crack found in a bracket may cause the ducting become unstable during a mission, and thus induces high cycle fatigue load on the overall major structures and shorten the structures life. From the economic standpoint, it is a cost saving strategy to replace brackets before they are completely damaged and malfunction due to replacing broken brackets mitigate the risk of damaging other major components, such as the ducting, which are more costly to replace. Besides, replacing a bracket before it completely breaks can avoid many engineering catastrophes and safe a lot of lifes. On the other hand, knowing the fatigue life of a component, a mechanic can plan the inspection interval accordingly.

Nickel-based alloy such as Inconel 718 and Inconel 625 are widely used in aerospace industry for ducting and brackets. However, according to Honnorat, only titanium alloys could satisfy the requirement and the increasing demand for high strength per weight materials that needed for a wide range of components [2]. According to the unknown author on World Wide Web, Wikipedia, many aircrafts use titanium due to their high tensile strength to density ratio, high corrosion resistance, fatigue resistance, high crack resistance, and ability to withstand moderately high temperatures without creeping [4].

Honnorat wrote in his paper in 1996 that jet engine designers use more and more titanium in both commercial and military projects, attaining contents as high as 30% of the total engine mass in the commercial and 40% in the military projects [2]. His statistic is consistent with recent data found on internet that about two thirds of all titanium metal produced is used in aircraft engines and frames [4]. In fact, many engine applications that use titanium include rotors, compressor blades, hydraulic system components, and nacelles. Among all the titanium-based alloys, according to Immarigeon et al, Ti-6-4 is by far the most widely used, accounting for almost half of all titanium used in aircraft [3]. Besides, he also mentioned Ti-6-2-4-2 is the other type of titanium-based alloy widely used in engines, which is stronger and more creep-resistant than Ti-6-4 [3].

According to Immarigeon et al, titanium-based alloys are widely used in engine applications because the material can increase the strength-to-weight ratio in structures and provide heat resistance with weight savings [3]. The material behavior under aggressive environment as well as impact loads make them attractive for aeroengine applications [2]. Their relatively low density decreases the magnitude of vibration problems [2]. However, the significant weight savings permitted by these titanium application developments generated specific drawbacks that needed particular technological developments. Among the most important concerns are the brittle inclusions, which are difficult to detect by non-destructive testing, and can initiate cracks and an early failure of the structures [2]. Materials imperfections due to manufacturing process, for example, void and impurities develop flaws that can cause a material become weak.

2. Problem Statement

Cracks often develop in the corner and at the edge of a structural member due to high stress concentration factor in those areas. If one can calculate the rate of crack growth, an engineer can schedule inspection accordingly and repair or replace the part before failure happens. Moreover, being able to predict the path of a crack helps a designer to incorporate adequate geometric tolerance in structural design to increase the part life. While producing durable, reliable and safe structures are the goals of every aerospace component manufacturer, there are technical challenges that are not easy to be solved. Given limited engine design space, engineers strive to optimize bracket geometry to produce high efficient and high performance engines that will operate at minimum weight and cost. Engineers often look to shave materials from bracket and design the thinnest possible brackets. Although this method could reduce weight, but brittle issues often found in bulk materials that could cause early failures in the structure. The focus of this paper is on assessing the structural integrity of a titanium-based alloy bracket, which contains physical flaws or material imperfections. The structural flaws or material imperfections include corner crack and surface crack. This paper will examine the stresses in the vicinity of the crack tip, compute the stress-intensity factors and compare it against material toughness to determine the influence of the crack on the bracket.

3. Theory

3.1 Linear Elastic Fracture Mechanics (LEFM)

For any homogeneous and isotropic material, stress surrounding the crack tip is analyzed using linear elastic material property. The method of linear elastic fracture mechanics assumes the plastic region near crack tip is so much smaller than the dimensions of the crack and the structural member. This is a very important concept, scientists and engineers call it small-scale yielding, for simplifying the stress analysis near crack tip. Assuming the geometry has very small displacement and the material is elastic, homogeneous and isotropic. The governing equations for linear elastic analysis are

1) Strain-displacement relationships:

$$\varepsilon_{xx} = \frac{\partial u_x}{\partial x} \qquad \varepsilon_{yy} = \frac{\partial u_y}{\partial y} \qquad \varepsilon_{xy} = \frac{1}{2}\left[\frac{\partial u_x}{\partial y} + \frac{\partial u_y}{\partial x}\right]$$ **Eq. (1) – (3)**

2) Stress-strain relationships:

i. For plane strain, where $\varepsilon_{zz} = \varepsilon_{xz} = \varepsilon_{yz} = \tau_{xz} = \tau_{yz} = 0$ **Eq. (4)**

$$\sigma_{xx} = \frac{E}{(1+\nu)(1-2\nu)}\left[(1-\nu)\varepsilon_{xx} + \nu\varepsilon_{yy}\right]$$ **Eq. (5)**

$$\sigma_{yy} = \frac{E}{(1+\nu)(1-2\nu)}\left[(1-\nu)\varepsilon_{yy} + \nu\varepsilon_{xx}\right]$$ **Eq. (6)**

$$\tau_{xy} = 2\mu\varepsilon_{xy} = \frac{E}{1+\nu}\varepsilon_{xy}$$ **Eq. (7)**

$$\sigma_{zz} = \nu(\sigma_{xx} + \sigma_{yy})$$ **Eq. (8)**

ii. For plane stress, where $\sigma_{zz} = \varepsilon_{xz} = \varepsilon_{yz} = \tau_{xz} = \tau_{yz} = 0$ **Eq. (9)**

$$\sigma_{xx} = \frac{E}{1-\nu^2}\left[\varepsilon_{xx} + \nu\varepsilon_{yy}\right]$$ **Eq. (10)**

$$\sigma_{yy} = \frac{E}{1-\nu^2}\left[\varepsilon_{yy} + \nu\varepsilon_{xx}\right]$$ **Eq. (11)**

$$\tau_{xy} = 2\mu\varepsilon_{xy} = \frac{E}{1+\nu}\varepsilon_{xy}$$ **Eq. (12)**

$$\varepsilon_{zz} = \frac{-\nu}{1-\nu}(\varepsilon_{xx} + \varepsilon_{yy})$$ **Eq. (13)**

3) Equilibrium equations:

$$\frac{\partial \sigma_{xx}}{\partial x} + \frac{\partial \tau_{xy}}{\partial y} = 0 \qquad \textbf{Eq. (14)}$$

$$\frac{\partial \sigma_{yy}}{\partial y} + \frac{\partial \tau_{xy}}{\partial x} = 0 \qquad \textbf{Eq. (15)}$$

4) Compatibility equation:

$$\left[\frac{\partial^2}{\partial x^2} + \frac{\partial^2}{\partial y^2}\right](\sigma_{xx} + \sigma_{yy}) = 0 \qquad \textbf{Eq. (16)}$$

Airy stress function, Φ, can satisfy all the governing equations and derive the stress fields near the crack tip.

$$\phi = \frac{K_I}{3\sqrt{2\pi}} r^{3/2}\left(\cos\frac{3\theta}{2} + 3\cos\frac{\theta}{2}\right) \qquad \textbf{Eq. (17)}$$

$$\frac{\partial^4 \phi}{\partial x^4} + 2\frac{\partial^4 \phi}{\partial x^2 \partial y^2} + \frac{\partial^4 \phi}{\partial y^4} = 0 \qquad \textbf{Eq. (18)}$$

Solving Eq. (?), the stress fields for Mode I are

$$\sigma_x = \frac{K_I}{\sqrt{2\pi r}}\cos\frac{\theta}{2}\left(1 - \sin\frac{\theta}{2}\sin\frac{3\theta}{2}\right) \qquad \textbf{Eq. (19)}$$

$$\sigma_y = \frac{K_I}{\sqrt{2\pi r}}\cos\frac{\theta}{2}\left(1 + \sin\frac{\theta}{2}\sin\frac{3\theta}{2}\right) \qquad \textbf{Eq. (20)}$$

$$\tau_{xy} = \frac{K_I}{\sqrt{2\pi r}}\cos\frac{\theta}{2}\cos\frac{3\theta}{2}\sin\frac{3\theta}{2} \qquad \textbf{Eq. (21)}$$

$$\sigma_z = \nu(\sigma_x + \sigma_y) \qquad \textbf{Eq. (22)}$$

$$\tau_{xz} = \tau_{yz} = 0 \qquad \textbf{Eq. (23)}$$

The displacement fields are

$$u = \frac{K_I}{G}\sqrt{\frac{r}{2\pi}}\cos\frac{\theta}{2}\left(1 - 2\nu + \sin^2\frac{\theta}{2}\right) \qquad \textbf{Eq. (24)}$$

$$v = \frac{K_I}{G}\sqrt{\frac{r}{2\pi}}\sin\frac{\theta}{2}\left(2 - 2\nu - \cos^2\frac{\theta}{2}\right) \qquad \textbf{Eq. (25)}$$

$$w = 0 \qquad \textbf{Eq. (26)}$$

3.2 Stress Intensity Factor (SIF)

Principal stresses do not account for all the fracture behaviors at the tip of a crack because the stress level could become infinity, which is not a real property of a loaded structure. As an alternative to describe the structural strength at the crack tip appropriately, stress-intensity factor, K, is a parameter to characterize "the stress field ahead of a sharp crack in a test specimen or a structural member." The parameter, K, is related to the nominal stress level (σ) in the structural member and the size of the crack (a), and has units of $ksi\sqrt{in}$ $(MPa\sqrt{m})$. According to Barsom, "all structural members or test specimens that have flaws can be loaded to various levels of K. This is analogous to the situation where unflawed structural or mechanical members can be loaded to various levels of stress, σ" [5].

The stress fields in the vicinity of crack tips can be categorized as Mode I: opening mode, Mode II: sliding and Mode III: tearing, which each of them is characterized by a "local mode of deformation" as illustrated in Figure 1. The opening mode, I, is related with local displacement in which the crack surfaces move directly apart (symmetric with respect to the x-y and x-z planes). The sliding mode, II, is related with local displacement in which the crack surfaces slide over one another perpendicular to the leading edge of the crack (symmetric with respect to the x-y plane and skew-symmetric with respect to the x-z plane). The tearing mode, III, is related with local displacement in which the crack surfaces slide with respect to one another parallel to the leading edge (skew-symmetric with respect to the x-y and x-z planes). Although these three modes can be superposed to "describe the most general case of crack tip deformation and stress fields" [6], but Mode I is the primary focus of this paper.

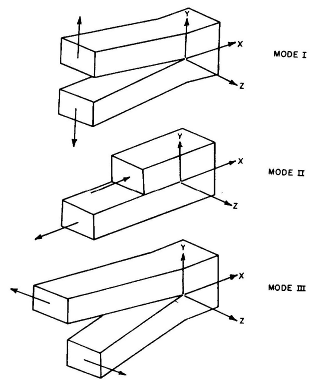

Figure 1 The three basic modes of crack surface displacements [5].

In general, stress-intensity factor depends on the stress induced on a structure, the crack size and the geometry of the crack. The stress-intensity factor equation for an embedded circular crack is given by [6]:

$$K_I = \frac{\sigma\sqrt{\pi a}}{\phi}\left(\sin^2\beta + \frac{a^2}{c^2}\cos^2\beta\right)^{1/4} \tag{1}$$

For surface crack, the stress intensity factor is

$$K_I = (1.12)\frac{2}{\sqrt{\pi}}\sigma\sqrt{a} \tag{2}$$

1.12 is the free surface correction factor. It is added for every free surface at which a crack might originate. If the crack occurs at the corner of a plate, as shown in Figure 2, the K_I expression would be [5]:

$$K_I = (1.12)(1.12)\frac{2}{\sqrt{\pi}}\sigma\sqrt{a} \tag{3}$$

K_I is increased by 1.12 [5] because there are two free-surface corrections for a corner crack.

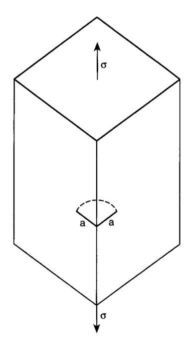

Figure 2 Circular corner crack [5].

4. Methodology

Engineers strive to optimize brackets geometry by designing the thinnest possible brackets because this approach not only reduce engine weight but also reduce the risk of brittle structure often found in bulk materials. Being able to determine the rate of crack growth, an engineer can schedule inspection accordingly and repair or replace the part before failure happens. Being able to predict the path of a crack helps a designer to incorporate adequate geometric tolerance in structural design to increase the part life. The mechanics of crack analysis include CAD model creation, stress analysis, flaw implementation, crack propagation, stress analysis of cracked model and interpretation of results. Carter, Wawryznek and Ingraffea have developed a time saving method to replace the tedious and repetitive work of crack growth simulation, called FRANC3D [8]. However, FRANC3D is a development program that has some limitations in stress analysis; therefore, other commercial software such as ANSYS must be used as complement.

The software for stress analysis is ANSYS Release 11.0. It is a popular code used by many experts in various industries for finite element analysis. The author chose ANSYS for its compatibility with FRANC3D Version 5.0. Dr. Paul Wawryznek developed the early FRANC codes in Cornell Fracture Group in to nucleate and propagate crack in a structure; and then compute stress intensity factor. Today, his student in the same group continues to research and update the codes.

4.1 CAD Model and Material

Michael Thomas contributed the bracket geometry used in his prior work to this study. In addition, the boundary condition chosen by Thomas for his optimum bracket research was applied to the bracket in this study [7]. At the base of the bracket, one end is clamped in all degree of freedom, while the other end is a slider. The bracket is pulled downward from the mid-section of the base and is pulled to the right at the top corner, see Figure 3.

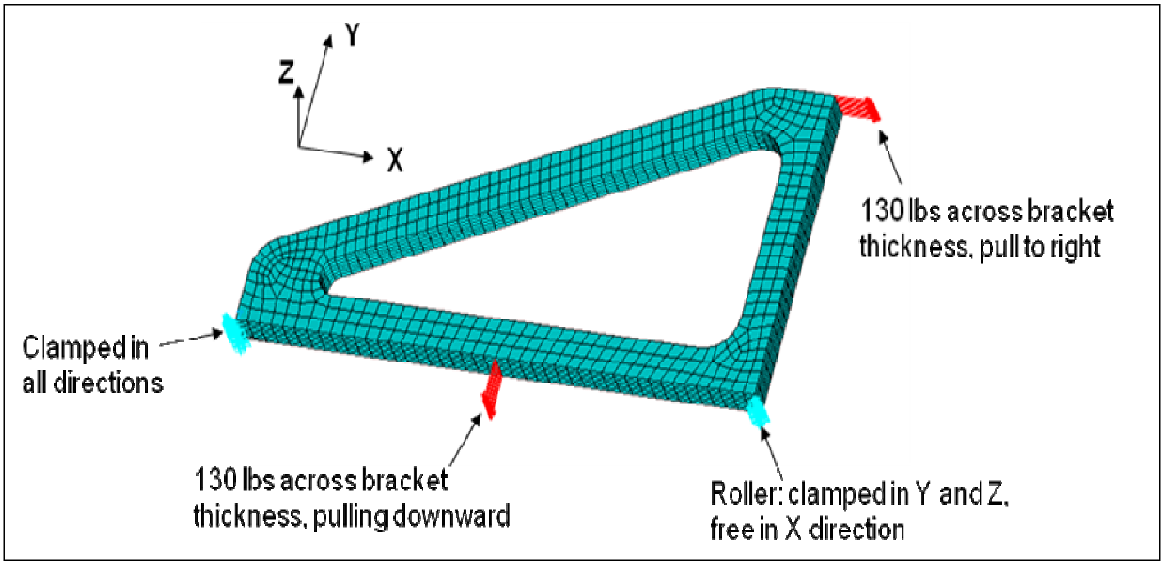

Figure 3 The boundary conditions of the unnotched bracket.

Among all the titanium-based alloys, according to Immarigeon et al, Ti-6Al-4V is by far the most widely used, accounting for almost half of all titanium used in aircraft because the material can increase the strength-to-weight ratio in structures and provide heat resistance with weight savings [3]. However, the significant weight savings permitted by these titanium application developments generated specific drawbacks that needed particular technological developments. Among the most important concerns are the brittle inclusions, which are difficult to detect by non-destructive testing, and can initiate cracks and an early failure of the structures [2]. Materials imperfections due to manufacturing process, for example, void and impurities develop flaws that can cause a material become weak. For that reasons, the material chosen for study is Titanium-6Al-4V and the properties are summarized in Table 1.

Material Properties		Comments
Density	0.160 lb/in³	
Tensile Strength, Ultimate	170000 psi	
Tensile Strength, Yield	160000 psi	
Elongation at Break	10.00%	
Modulus of Elasticity	16500 ksi	Average of tension and
Compressive Yield Strength	155000 psi	
Poissons Ratio	0.33	
Fatigue Strength	23200 psi	K_t (stress concentration factor) = 3.3
	@# of Cycles 1.00e+7	
	102000 psi	Unnotched
	@# of Cycles 1.00e+7	
Fracture Toughness	39.1 ksi-in½	
Shear Modulus	6380 ksi	
Shear Strength	110000 psi	Ultimate shear strength

Table 1 Material properties of Titanium-6Al-4V.

4.2 Analysis Procedure

The very first step of analysis was to perform finite element stress analysis on the unnotched bracket to determine stress distribution across the entire bracket, and then to identify the weakest point or high stress region in the bracket. Michael R. Thomas, who created the geometry, for his research paper, in a commercially available software, contributed the bracket CAD file [7]. The bracket CAD file was parasolid, which was compatible with ANSYS, therefore the author meshed the bracket in ANSYS environment. The author also constructed Ti-6Al-4V stress-strain curve based on the data in Table 1 using ANSYS graphic user interface (GUI). The author meshed the bracket with element type Solid95, 20-node, because it is the only type of element compatible with FRANC3D. After the author applied boundary conditions to the bracket as shown in Figure 3, she set ANSYS to perform single load step static stress analysis on the bracket. The finite element model of the unnotched bracket had 2828 elements and 12342 nodes, so the computing time was approximately fifteen minutes or less. Later, in ANSYS postprocessor, the author identified the most highly stressed region in the bracket, point A in Figure 4, for implementing initial crack. At last, ANSYS wrote a database DB file (.cdb) for FRANC3D crack growth analysis.

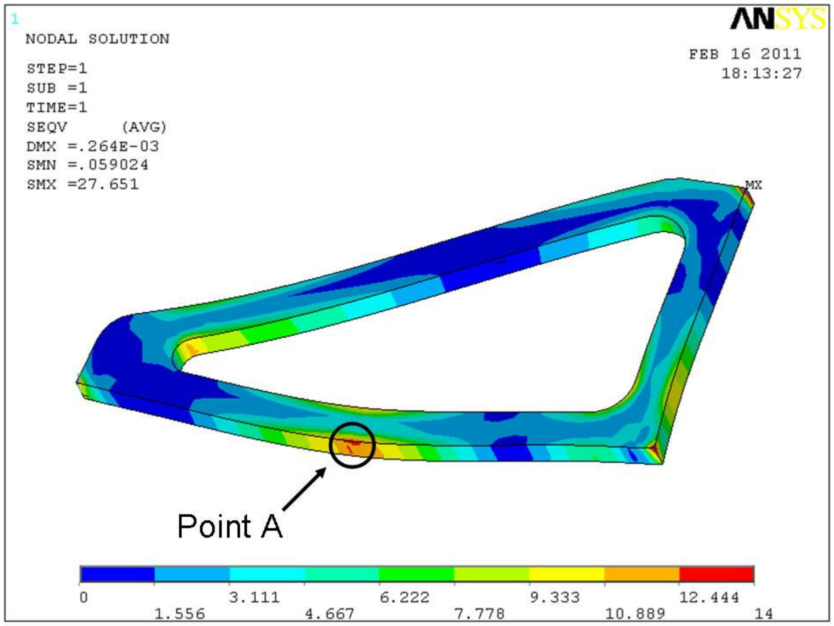

Figure 4 Stress distribution of the unnotched bracket (Von Mises).

Step two of analysis was to implement initial crack in the structure by creating basic geometry of the crack. The author first opened the .cdb file written in step one, in FRANC3D. Next the author implemented an initial crack in the structure by creating a circular crack of two-inch radius, and positioning the crack at the high stressed region identified in step one, or point A in Figure 4. One quarter of the circular crack was put at the edge to simulate corner crack. For comparison study, half of the circular crack was placed at the center of the material to simulate surface crack. This method was proposed by Nishioka, "The actual flaw from which fracture is initiated in a structural component, can be approximated, often by an ellipse or a part of an ellipse" [9]. After that, FRANC3D automatically generated finer meshes locally around the crack where the existing mesh would not constrain how the new mesh was formed [10]. FRANC3D is an automated program, which "delete automatically all the elements around the predicted new crack-tip location, insert crack-tip elements of the proper shape and number, and then create a transition mesh to fill the area between these elements and the unmodified portion of the mesh… This insures that the mesh around the new crack configuration will not be influenced by the original meshing of the structure." [10]. At last, the author used FRANC3D graphic user interface to create input file (.macro), a text file, which was readable by ANSYS, for stress analysis.

Step three of analysis was to perform stress analysis of the notched bracket produced in previous step. FRANC3D wrote all the procedure of running load step analysis and post-processing the results in the text file (.macro). Therefore, once the notched bracket from step two was brought into ANSYS by reading in the text file (.macro), ANSYS would generate a result file (.fdb) at the end of the analysis. It is a binary file, which only FRANC3D can read, to compute stress-intensity factors and extend the crack. Wawrzynek described the process of stress-intensity factors computation and the mechanism of crack propagation in his paper, "The displacements of the nodes along the crack-face are used to compute the stress-intensity factors for the crack-tip. These stress-intensity factors in conjunction with a propagation angle criterion…are used to determine the direction of crack propagation… Crack propagation proceeds by first deleting elements around the new and old crack-tip. A heuristic algorithm is used to determine which elements and the number of elements to be deleted. The crack is then extended and a rosette of quarter-point singular elements are placed around the new crack-tip" [10].

Step four of analysis was to propagate the crack to the critical length in multiple iterations. ANSYS generated DB input file (.cdb) and result file (.fdb) during static stress analysis, which both files must be available in the directory of FRANC3D execution file, to propagate the crack in FRANC3D. In every iteration, the author used default value for the crack tip size. Then the program computed stress-intensity factors based on the stress result (.fdb) and the current crack length. The author repeated steps three and four to continue propagating the crack.

Although this paper applied LEFM analysis method, FRANC3D is a sophisticated tool that also can perform nonlinear analysis. However, singularity exists in the plastic region at the crack tip when LEFM theory is not applied. Therefore, FRANC codes must meet two requirements to resolve the singular stress at the crack tip: elements size and number. Wawryznek wrote [10],

> (1) Size of elements: when generating a portion of a finite element mesh it is easier to generate elements which are all about the same size. The quarter point elements, however, usually have to be smaller than the other elements in the mesh to provide accurate estimates of the stress-intensity factors... Quarter-point elements that are large enough to model the region where the singular stress field dominates but small enough so that they

are not used to model the region where the singular stress field does not dominate.

(2) Number of elements: the mesh must be able to model the circumferential distribution of stress around a crack-tip. The circumferential distribution of stress is characterized by the product of trigonometric functions. This stress distribution will be modeled in a piecewise linear fashion which the T6 elements are capable of reproducing. As the number of elements is increased, one obtains a more faithful representation of the stress distribution. However, if too many elements are used around the crack-tip, the aspect ratio of the elements increases and their performance deteriorates.

To meet these two constraints FRANC employs a method of subdivision in the crack-tip elements…a rosette of crack-tip elements that would be automatically inserted by the program. Each of these triangular elements can be subdivided into a singular triangular element and a quadrilateral element. This process can be repeated to provide crack-tip elements of the proper size and a smooth transition from the crack-tip elements to the rest of the mesh.

5. Results

FRANC3D remeshed the entire bracket geometry when implementing initial crack by turning brick elements into tetrahedral elements. During the crack propagation phase, FRANC3D remeshed the area surrounding the crack, instead of the entire geometry, as shown in Figure 5 and Figure 6. After two load steps of crack propagation, about 45443 elements were added to the corner crack model and 107117 elements were added to the surface crack model. Table 2 summarizes the number of elements and nodes in each finite element model.

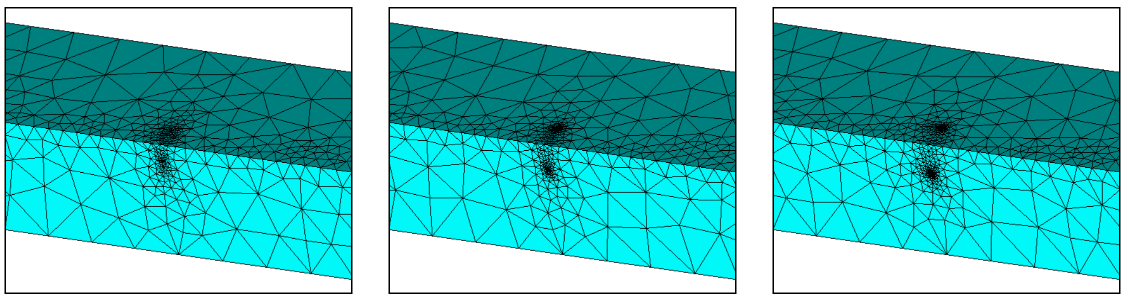

(5a) Initial crack. (5b) Crack growth load step 1. (5c) Crack growth load step 2.

Figure 5 Corner crack propagation.

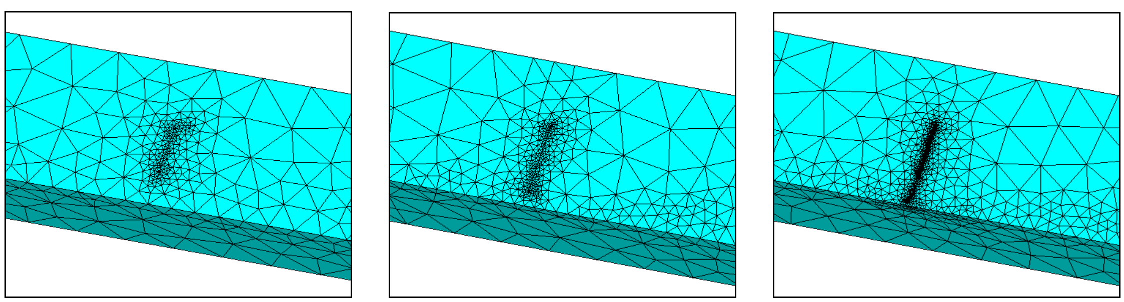

(6a) Initial crack. (6b) Crack growth load step 1. (6c) Crack growth load step 2.

Figure 6 Surface crack propagation.

Description of Bracket	Number of Elements	Number of Nodes
Unnotched	2828	12342
Corner Crack - Initial	33264	52611
Corner Crack Growth - Load Step 1	40517	63847
Corner Crack Growth - Load Step 2	48271	75337
Surface Crack - Initial	26333	43628
Surface Crack Growth - Load Step 1	36277	59464
Surface Crack Growth - Load Step 2	109945	173483

Table 2 Number of elements and nodes.

5.1 Stress Field Around Initial Crack

Figure 7 shows the stress fields surrounding the initial cracks for corner crack and surface crack, respectively. Stress in the bracket top right corner has singularity due to point load, so its effect on the structure is not real and can be ignored. After two load steps of crack propagation, the maximum values in the vicinity of crack tip are **TBD** psi and **TBD** psi for corner crack and surface crack, respectively. They are below the yield stress and fatigue stress.

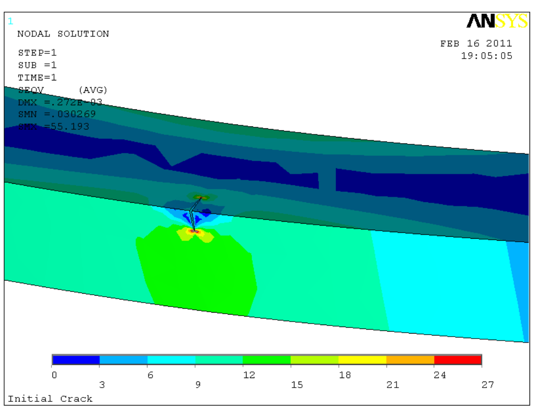

(7a) Corner crack stress field.

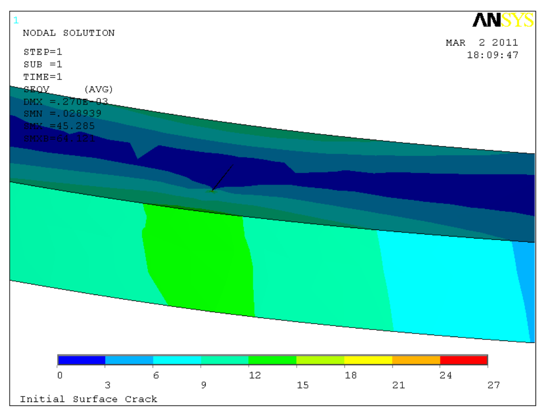

(7b) Surface crack stress field.

Figure 7 Stress field around initial crack.

5.2 Stress Field Around Propagated Crack

Figure 8 shows the stress fields surrounding the propagated cracks for corner crack and surface crack, respectively. Stress in the bracket top right corner has singularity due to point load, so its effect on the structure is not real and can be ignored. After two load steps of crack propagation, the maximum values in the vicinity of crack tip are **TBD** psi and **TBD** psi for corner crack and surface crack, respectively. They are below the yield stress and fatigue stress.

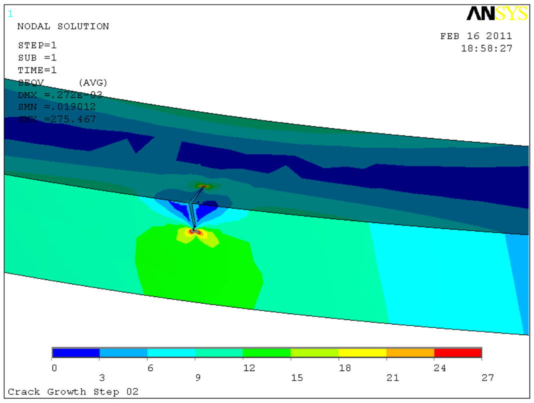

(8a) Corner crack stress field.

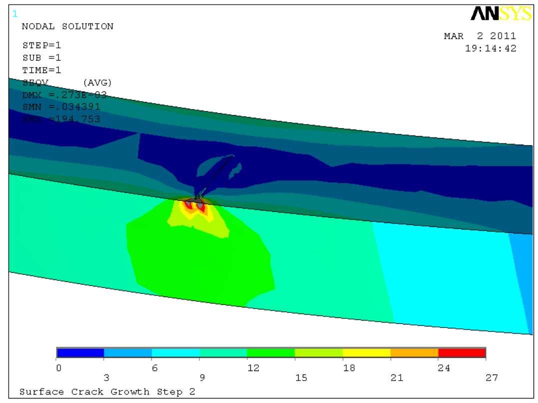

(8b) Surface crack stress field.

Figure 8 Stress field around propagated crack.

5.3 Stress Intensity Factor

The Mode I stress-intensity factors for corner crack and surface crack are shown in Figure 9. The highest value for corner crack is 25.2 $psi\sqrt{in}$ and for surface crack is 31.2 $psi\sqrt{in}$. They are below the material's fracture toughness.

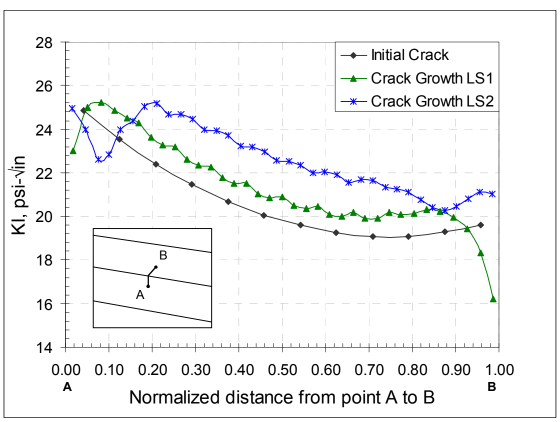

(9a) KI of corner crack.

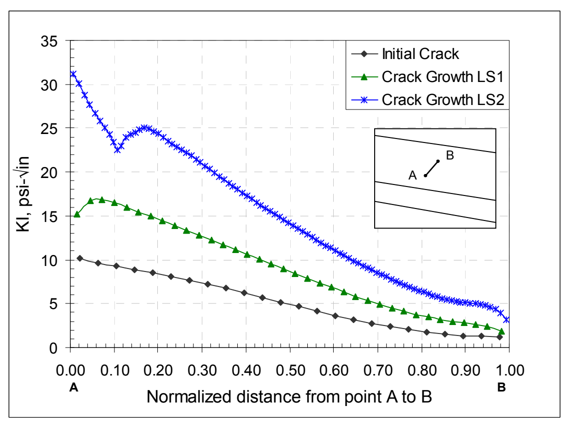

(9b) KI of surface crack.

Figure 9 Mode I stress-intensity factors.

6. Discussion and Conclusions

There must be at least six elements across the bracket thickness to insert new crack elements in FRANC3D, for this reason, brick elements were used to ensure enough elements were present across the thickness while keeping the total number of elements in the geometry small. However, since FRANC3D deployed "tetrahedral volume meshing algorithm" [8] to implement initial crack and propagate existing crack, the program did a one-time remesh to the entire bracket geometry to turn brick elements into tetrahedral elements. In subsequent crack growth procedures, FRANC3D did local remesh to the elements around the crack; therefore, area around the crack has finer mesh than area further away from the crack. In general, once the geometry was populated with tetrahedral elements, areas far from the crack had the same nodes pattern between one load step and other load step. New crack length was calculated based on a polynomial series, where the variable of the series is the displacement of the node at the crack tip [8]. Crack was propagated and reanalyzed until a desire cumulated crack length is achieved. The analysis results show that the static stress and KI SIF at one end of the crack, point A, is higher than the other end, point B, see Figure 7, Figure 8 and Figure 9, because point A is at the face where the force is applied. For both corner crack and surface crack modelings, the results also show the static stress is below yield strength. The Mode I stress intensity factors for both crack modelings are also below the material's fracture toughness. Therefore, the bracket can tolerate small crack in the structure. The fatigue strength of the structure is recommended to be assessed in the future.

7. References

[1] Unknown. FRANC3D & ANSYS Tutorial. September 2010. http://www.fracanalysis.com/Franc3D_Documentation (accessed February 5, 2010).

[2] Honnorat, Yves. "Issues and breakthrough in manufacture of turboengine titanium parts." Materials Science and Engineering A213, 1996: 115-123.

[3] Immarigeon, J-P., Holt, R.T., Koul, A.K., Zhao, L., Wallace, W. and Beddoes, J.C., Lightweight Materials for Aircraft Applications, NRC Institute for Aerospace Research, 1995.

[4] Unknown. Titanium. n.d. http://en.wikipedia.org/wiki/Titanium (accessed January 12, 2011).

[5] Barsom, John M. and Rolfe, Stanley T., Fracture and Fatigue Control in Structures: Application of Fracture Mechanics, Philadelphia, 1999.

[6] Paris, C.P. and Sih, G.C., "Stress Analysis of Cracks," in Fracture Toughness Testing and Its Applications, ASTM STP 381, American Society for Testing and Materials, Philadelphia, 1965.

[7] Thomas, Michael R., Shape and Topology Optimization of Brackets using the Level Set Method, Hartford CT, 2010.

[8] Carter, B.J., Wawrzynek, P.A. and Ingraffea, A.R., Automated 3D Crack Growth Simulation, Cornell Fracture Group, 2003.

[9] Nishioka T. and Atluri S.N., Analytical Solution For Embedded Elliptical Cracks, And Finite Element Alternating Method For Elliptical Surface Cracks, Subjected to Arbitrary Loadings, Engineering Fracture Mechanics Vol. 17, No.3, pp. 247-268, 1983.

[10] Wawrzynek, P.A. and Ingraffea, A.R., An Interactive Approach To Local Remeshing Around A Propagating Crack, Finite Elements in Analysis and Design 5 (87-96), 1989.